JOURNAL OF THEORETICAL AND APPLIED MECHANICS
49, 3, pp. 685-704, Warsaw 2011

EFFICIENT AND LOW COST PZT NETWORK FOR DETECTION AND LOCALIZATION OF DAMAGE IN LOW CURVATURE PANELS

Nicolae Constantin, Ştefan Sorohan, Mircea Găvan

The University "Politehnica" of Bucharest, Laboratory for Integrity Evaluation of Composite Structures, Bucharest, Romania; e-mail: nicolae.constantin@mechstruct.pub.ro

Vladimir Raeţchi

Vovasonic SRL, Bucharest, Romania

The paper presents results obtained in creating an efficient inspection technique, based on the Lamb wave method, by using a powerful central signal generator, a network of receivers and a simple triangulation algorithm for detecting and localizing a defect/damage in metallic or composite panels. This is intended to be done in two variants: (i) with a fixed central PZT patch able to blast powerful omnidirectional waves of the desired frequency, shape and duration and (ii) with a variable angle mobile actuator able to generate powerful guided waves. The first variant is aimed for online monitoring, while the second, for field inspections. At this stage, only numerical simulations of the first variant have been made, with promising results in metallic panels.

Key words: Lamb wave, PZT patch, signal generator, triangulation

1. Introduction

Structural health monitoring (SHM) is a major domain in nowadays efforts meant to increase reliability of mechanical structures by detecting, localizing and characterizing defects/damage with good accuracy. The first two actions belong to global monitoring, the domain in which not many nondestructive (NDT) methods are competing, due to its intrinsic large scale character, which creates difficulties in scanning time, signal transmissibility and interference with noise, localization algorithms, online monitoring capabilities, etc. It seems that only vibration based and Lamb wave methods are promising to develop,

in various variants, truly operational global SHM methods, overcoming, by clever improvements, the above mentioned difficulties.

In recent years, the Lamb wave method has nourished great expectations concerning its long range efficiency and online capabilities. A huge progress happened in the application of this method, from the signal generation to the interpretation of received waves with PZT patches/wafers proving the most versatile, in single version or networks, with a really wide range of shapes, properties and mounting techniques (Cawley and Alleyne, 1996; Nieuwenhuis *et al.*, 2005; Giurgiutiu, 2008; Wang *et al.*, 2008). Applications to composite materials and structures, particularly regarding signal transmission and receiving, are still a serious challenge for researchers and end users (Nayfeh, 1991; Diaz Valdes and Soutis, 2000; Kessler *et al.*, 2000; Zhongquing *et al.*, 2006). Numerical simulations are still ahead the experiments (Moser *et al.*, 1999; Mace and Manconi, 2008; Sorohan *et al.*, 2007; Von Ende and Lammering, 2009), and the gap has to be reduced, in conditions when the research and technological efforts are continuing to move forward, towards higher accuracy in detecting, localizing and characterizing flaws, on the benefit of reliable SHM.

Accurate localization of defects or damage in composite panels is a very attractive goal, as it means a lot of time saving and, consequently, lower maintenance cost, higher efficiency of the entire exploitation and increased availability for a number of sensitive structures involving such parts, especially in the aerospace and naval industry. During recent years, the localization has come together with the detection, especially concerning low velocity impact events (De Stefano *et al.*, 2010; Paget *et al.*, 2010; Tsutsui *et al.*, 2010). But detection, which is the first step in SHM strategy, implies only outputs, needing just passive techniques and sensors. This feature enables the use of PZT or Fibre Bragg Grating (FBG) sensors, both allowing on-line SHM. The localization needs active interrogation, possible with actuators, like PZT patches and signal receivers, which may be again PZT patches or FBG. The all PZT variant makes possible the alternate use as an active or passive transducer of each PZT patch in some diagnosis techniques (Burgos *et al.*, 2010).

The localization poses another big challenge for researchers and practitioners as well: best/optimal placement of sensors and actuators, in order to reduce/minimize errors. Several methods have been proposed for establishing the most effective distribution for getting comprehensive information upon the integrity of the monitored structure (Padula and Kincaid, 1999; Papadimitriou, 2005). In spite of using modern approaches, like Artificial Neural Networks and Genetic Algorithms for sophisticated but not yet very effective strategies, it is admitted that the best solution for damage location relies still

on the experience of the person in charge with SHM procedures (De Stefano *et al.*, 2010).

Yet, interesting ideas for sensor networking and associated algorithms for damage localization are presented in Tua *et al.* (2004), Lu *et al.* (2006), Diamanti *et al.* (2007), Ihn and Chang (2009), Ostachowicz *et al.* (2009), Cheng *et al.* (2010), Ricci *et al.* (2010), Wandowski *et al.* (2010).

The localization process is using *pitch-catch* and *pulse-echo* techniques. The first is applied when continuous or long signals are generated, the analysis of the received signal giving information about the flaw presence, but also about the damage level. It needs a larger number of sensors and more time for the interrogation and analysis process, implying, in recent approaches, the evaluation of the damage index (DI) (Ihn and Chang, 2009; Ostachowicz *et al.*, 2009; Cheng *et al.*, 2010; Wandowski *et al.*, 2010), somehow equivalent with the modal assurance criterion (MAC), used in vibration based methods that can go together with the Lamb wave method when the range of frequencies is large enough (Ricci *et al.*, 2010). The second technique was so far used merely for damage localization, the severity of the flaw being a precondition for getting a "readable" echo signal.

The paper presents results obtained in creating an efficient inspection technique, by using a powerful central signal generator and a small, but wisely distributed network of receivers. With a simple algorithm, detecting and localizing a defect/damage can be made quite easily.

2. Monitoring of metallic panels

The first model taken into consideration was a $700 \times 500 \times 1.59\,\mathrm{mm}^3$ Al panel, clamped on the boundary, with a central solidly bonded PZT, 6.4 mm in diameter (Fig. 1). This PZT – position 1 on the panel – is a Lamb wave actuator with a similar thickness to that of the inspected plate. In all points shown on the panel are collected signals due to the propagation of the original wave, including the point of actuation. Analysis of these signals are meant to indicate which should be the most relevant positions for placing sensors, so that location of damage can be reliably performed. These sensors are considered to be thin enough for having a negligible interference with the waves.

The numerical model was analyzed with LS-Dyna code, by the explicit integration approach. By DOF conditioning, a 2D plane stress FE model was created, in which only S0 waves can propagate at the rather low adopted

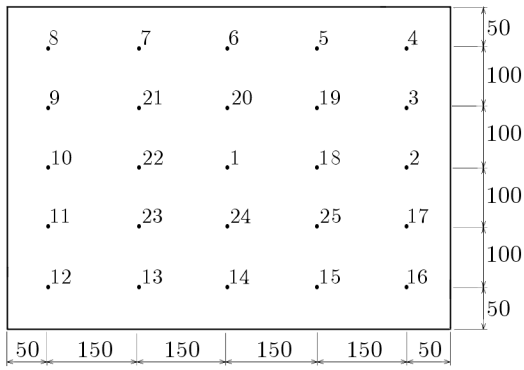

Fig. 1. Scheme of actuation PZT wafer and virtual sensors topology on the inspected Al panel

frequencies. This numerical strategy allowed important savings in terms of the code running time.

Wave actuation was performed through the structural only models (Constantin *et al.*, 2006), which is a short cut from the more sophisticated multiphysics approach. Accordingly, the forces resulted from the piezoelectric effect are distributed on the boundary of the PZT patch (Fig. 2), being transferred to the panel by the strong PZT-substrate interface. Such a model keeps the basic features of the true mechanism of Lamb wave generation with much less computational effort. That simplification had to balance the vast mesh dimension – 351 273 nodes and 350 072 finite elements – imposed by the need to use small elements able to accurately drive the generated waves. A less fine mesh produced propagation anisotropy, totally inappropriate for the intended analysis.

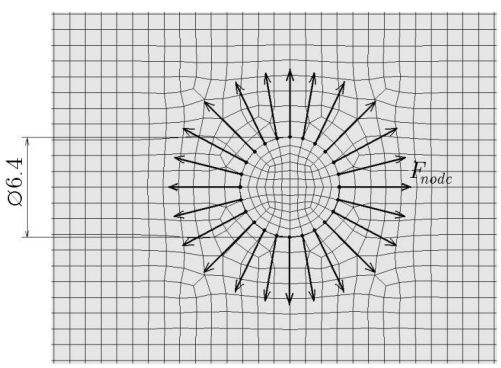

Fig. 2. Distribution of forces resulting from piezoelectric effect and strong PZT/substrate interface

The basic dispersion curves obtained for an Al plate of 1.59 mm in thickness are presented in Fig. 3. The 400 kHz frequency was chosen for the actuation signal as this corresponds to a small wave length well covered by the mesh, and to the still non-dispersive propagation of the S0 mode. The main characteristics of the S0 mode at this frequency, extracted from the dispersion curves in Fig. 3 are: wave length $\lambda = 13.4\,\text{mm}$, group velocity $v_g = 5290\,\text{m/s}$.

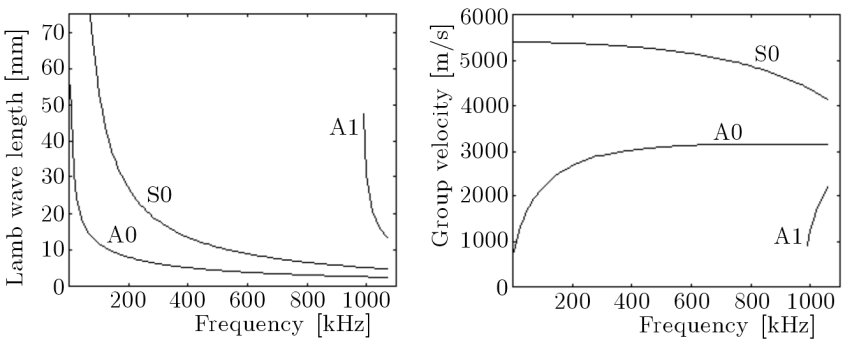

Fig. 3. Main dispersion curves for the Al plate model

The signal was actuated by a Hanning windowed force function imposed in phase to all forces distributed on the PZT boundary

$$F_{node}(t) = \frac{1}{2}F_0\Big(1 - \cos\frac{2\pi f_0 t}{n_0}\Big)\sin(2\pi f_0 t) \tag{2.1}$$

with the force amplitude $F_0 = 15.9\,\text{N}$, number of cycles $n_0 = 3$ and central frequency $f_0 = 400\,\text{kHz}$. The length of the excited signal, controlled by n_0, was chosen in that medium range in order to avoid interference with reflected signals and excitation of parasite frequencies.

Apart the pristine reference Al panel, two damaged variants were considered (Fig. 4). Each damaged zone, 32 mm in diameter, considerably over the 13.4 wave length of the blast signal, was simulated by decreasing 1000 times the Young modulus for the material of the elements inside that area. The propagation of the S0 Lamb wave created by the blast signal and its interference with the damaged areas is presented in Fig. 5a and 5b, for the two damage configurations, respectively.

The reception of signals in each point was analyzed in the idea that a true sensor is placed there, thin enough not to distort the wave. It was considered that the voltage in the sensor is proportional with the resultant of the two components of the nodal displacement and has the sign of their sum.

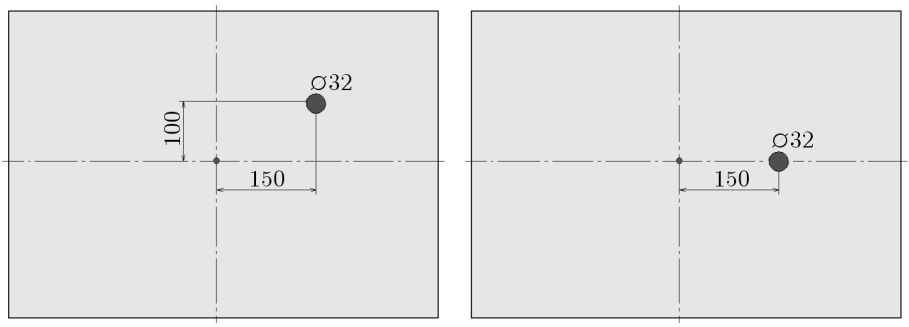

Fig. 4. Damage configurations: (a) single quarter-diagonal (*damage 1*), (b) single quarter-horizontal (*damage 2*)

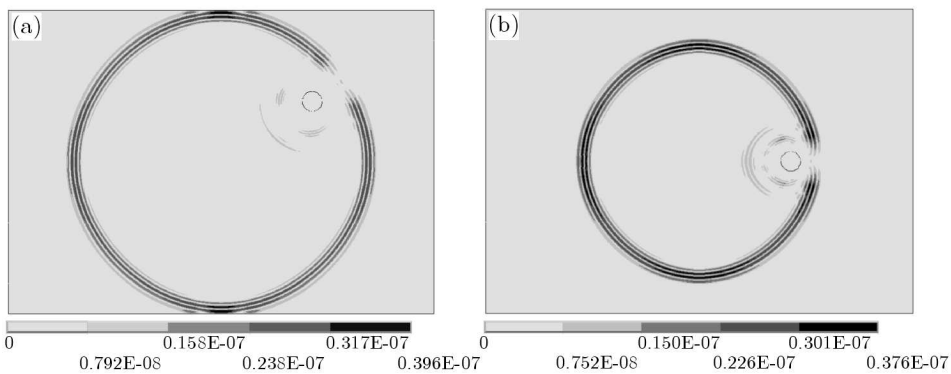

Fig. 5. Propagating wave at: (a) $t = 50\,\mu$s in the Al panel with quarter-diagonal damage, (b) $t = 40\,\mu$s in the Al panel with quarter-horizontal damage

Consequently, the instantaneous signal S, obtained instead of the voltage in the numerical model was given by the function

$$S = \operatorname{sgn}(u+v)\sqrt{u^2+v^2} \tag{2.2}$$

where u is UX and v is UY, the displacements given by the FE model.

Assuming that the actuator placed in central position 1 acts like a sensor after it blasts the actuation signal, the received signals in the plate having *damage 1* or *damage 2* are presented in Fig. 6, both representing echo signals from each damage.

The signals received by the sensor placed in point 2 are presented in Fig. 7. It has to be mentioned that the direct signal crossing *damage 2* area is significantly attenuated, with direct influence on the signal reflected from the right hand boundary. It is to be outlined that the echo from *damage 1* is marked only by a very weak noise after the direct signal.

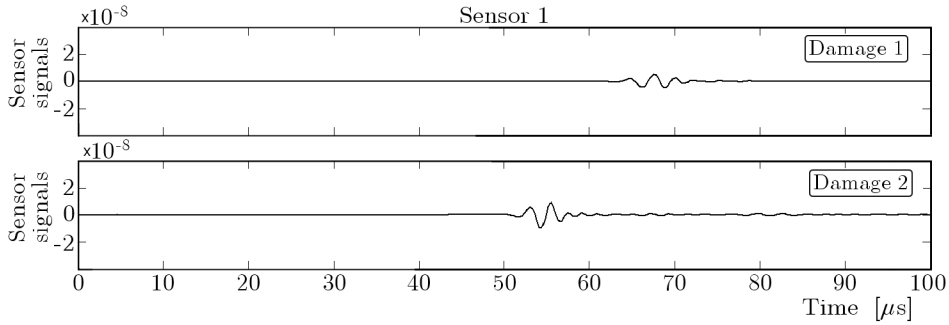

Fig. 6. Signals received in point 1 of the Al panel

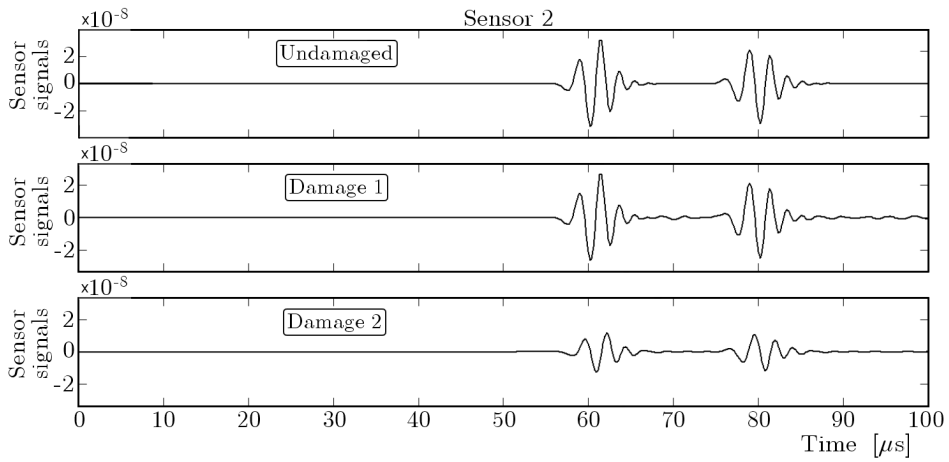

Fig. 7. Signals received in point 2 of the Al panel

The signals received by the sensor placed in point 3 are presented in Fig. 8. There is almost no difference between the three recorded signals, meaning that the echo signals produced by any of the damaged areas are not reflected in the direction of that sensor. The two powerful reflected signals are coming from the panel boundaries: the first, stronger, from the neighbouring right hand one, immediately followed by the second, weaker, from the top one.

The signals received in point 4 (Fig. 9) put in evidence a more irregular pair of reflected signals from the close boundaries and an attenuated direct signal, due to the crossing of *damage 1* zone.

The signals received in point 5 are almost identical to those received in point 3 (see Fig. 8), translated with the extra-time produced by the extra-distance to actuation point 1.

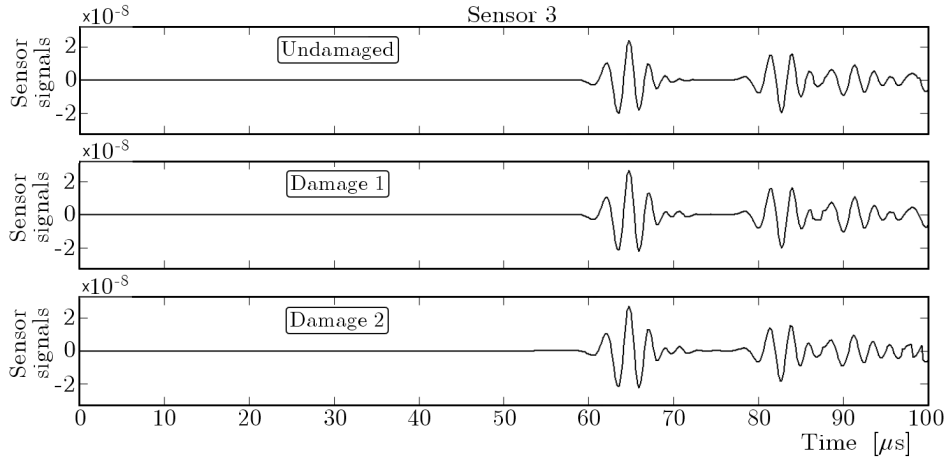

Fig. 8. Signals received in point 3 of the Al panel

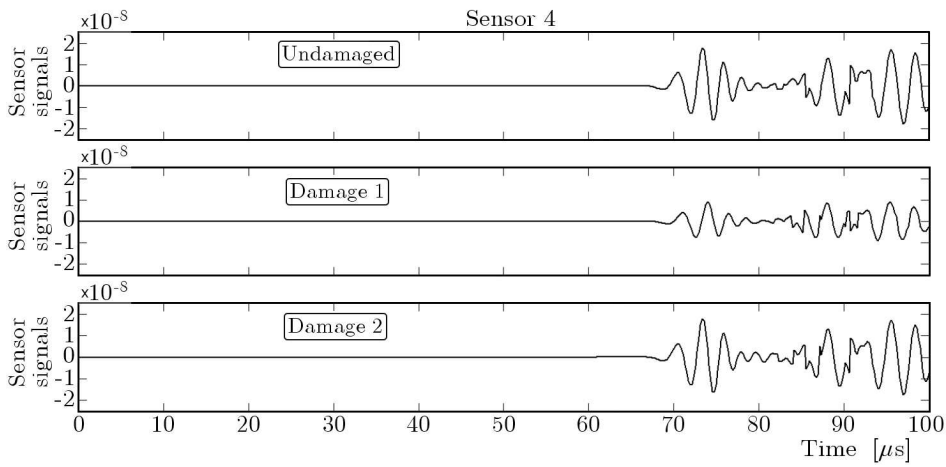

Fig. 9. Signals received in point 4 of the Al panel

The signals received in point 6 (Fig. 10) are really interesting. When the panel is considered damaged only in point 19 (*damage 1*), the weak, but undeniable echo signal from that damage is received immediately after the powerful signal reflected from the top boundary. A second echo signal from the same damage (see Fig. 5a), is recorded at the end of the $100\,\mu$s time window. When the panel is considered damaged only in point 18 (*damage 2*), a clearly individualized echo signal from that area is recorded after the powerful signal reflected from the top boundary. The next echo signal is coming soon (see Fig. 5b).

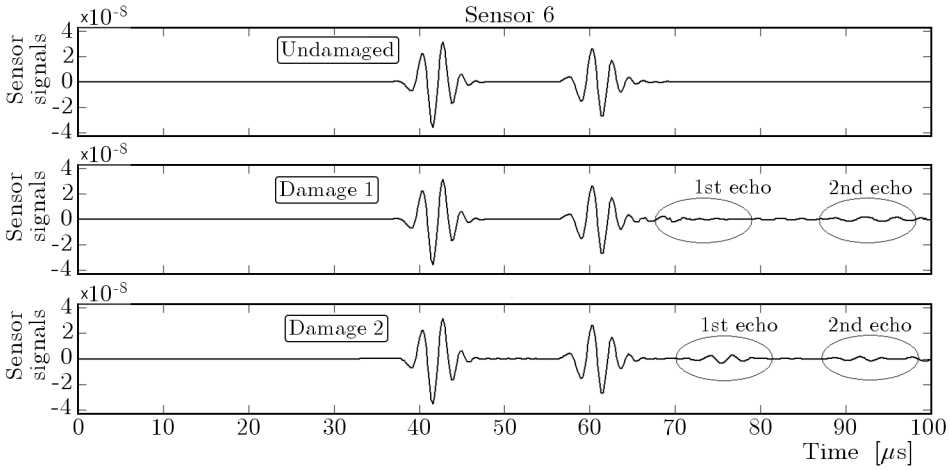

Fig. 10. Signals received in point 6 of the Al panel

The next interesting signals are recorded in point 14 (Fig. 11). The powerful signal reflected from the bottom boundary is followed by the first echo signal from *damage 1*, due to the bigger distance versus the time window, but by both echo signals from *damage 2*.

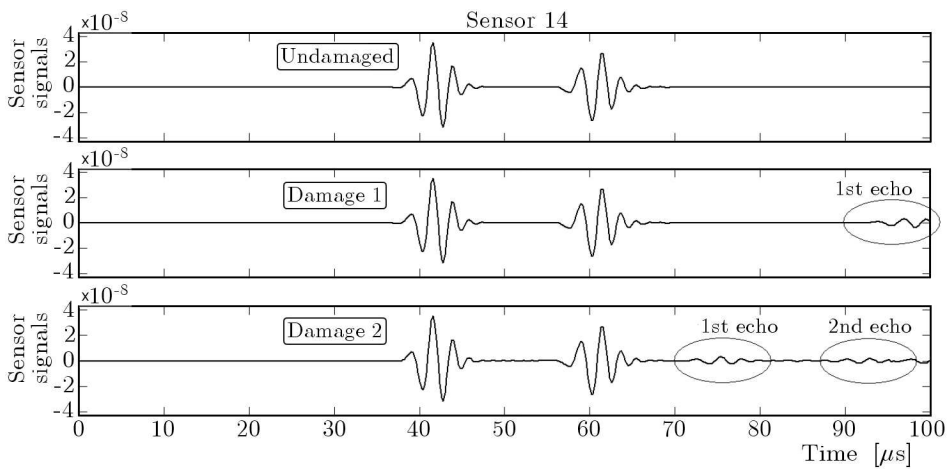

Fig. 11. Signals received in point 14 of the Al panel

The last interesting signals to be shown here are those recorded in point 15 (Fig. 12). The two neighbouring reflected signals from the bottom and right hand borders are followed by the echo signals produced by the damaged areas. For the panel with *damage 2*, closer to point 15, both echo signals are obtained in the chosen time window.

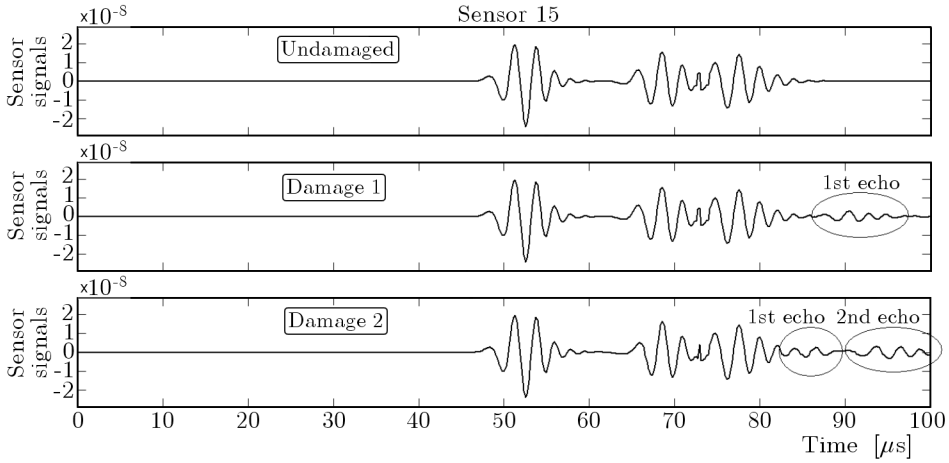

Fig. 12. Signals received in point 15 of the Al panel

Reviewing the recorded signals presented above, some important issues must be retained:

1. The damaged areas are reflecting detectable echo signals only in the forward half-plane with respect to the incident waves.
2. Waves passing in the close neighbourhood of the damaged areas are not distorted.
3. Waves crossing the damage are considerably attenuated.
4. More than one powerful reflected signal from the panel boundaries may endanger clear record of the much weaker echo signals from the damaged areas.

As only by pure coincidence the damage can be right on the line between the actuator and the sensor, only the echo signals can be used in locating the damage. Having in view the results, we propose the algorithm described below.

Looking at Fig. 6, the time of flight (ToF) for the return signal between point 1 and *damage 1* was about $68\,\mu$s, with the group velocity of 5290 m/s. Then, *damage 1* is located at $68 \times 10^{-6} \times 5290 \times 10^3 : 2 = 180$ mm, somewhere on the circle with that radius (Fig. 13). The echo signal from *damage 1* arrives at the sensor in point 6 in about $68\,\mu$s from the actuation moment (see Fig. 10), but the time for covering the distance from *damage 1* to point 6 must be obtained by deducting from the total ToF the time in which the blast signal arrives at the damaged area and ignites the echo signal: $68 - 68 : 2 = 34\,\mu$s.

Accordingly, *damage 1* must be somewhere on a circle with the radius $34 \times 10^{-6} \times 5290 \times 10^3 = 180$ mm. In fact, it will be in one of the two points of intersection between the circles with the centre in point 1 and in point 6. Following the same steps for the sensor in point 14 as for the sensor in point 6, one can easily find that *damage 1*, which produced the first echo signal after about 97 μs (see Fig. 11), must be on a circle with a radius of about 335 mm around point 14. The intersection of this circle with the previous two conveys to the same two points (Fig. 13) as all three sensors acquiring the echo signals are placed on a line. Repeating the procedure for the sensor in point 15, one finds that *damage 1*, which produced this time the first echo signal after about 91 μs (see Fig. 12), must be on a 300 mm radius circle around point 15. This circle has only one common point with the circles centred in points 1 and 6, that point being the centre of *damage 1*. This can be considered a form of "triangulation", allowing one to localize the point by intersecting circles centred in the three corners of a triangle. One can see that the double solution arises not only in the case when the triangle is degenerated to a line, but also in the very particular case when the triangle is isosceles and the damage lies on its axis of symmetry.

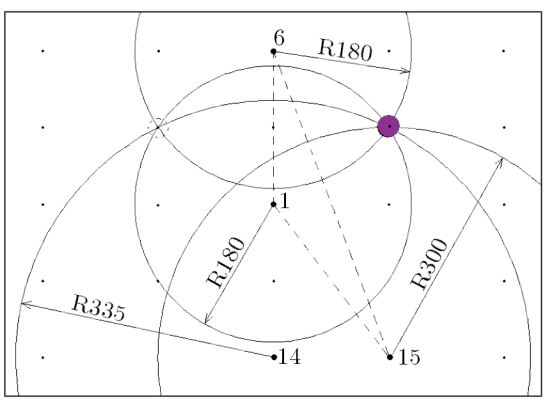

Fig. 13. Damage localisation by "triangulation" variants

Following a similar algorithm, one can easily find that *damage 2* lies at the intersection between the circles with centre in point 1 and a radius of 150 mm, with centre in point 6 and a radius of 250 mm and with centre in point 15 and a radius of 200 mm.

3. Monitoring of composite panels

The second model taken into consideration was a $350 \times 250 \times 2.16\,\text{mm}^3$ cross-ply composite panel (Fig. 14), with $[0/90/0]_s$ layoff formula, with the properties presented in Table 1. In the same figure, the position of the actuator, distribution of the sensors and damaged areas are presented.

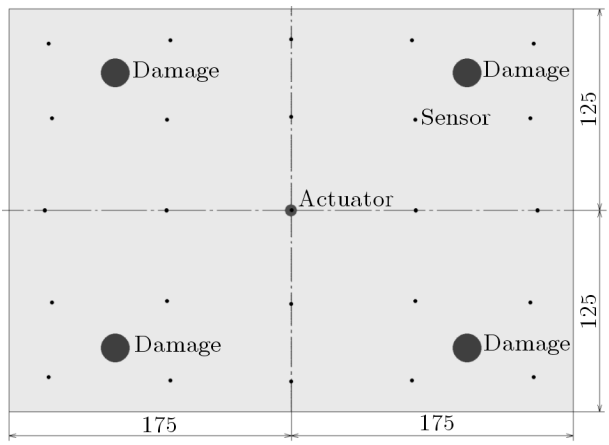

Fig. 14. Full model of the composite panel

Table 1. Engineering constants of the composite plate layers

Young's modulus [GPa]	Poisson's ratio (major)	Shear modulus [GPa]	Mass density [kg/m^3]
$E_1 = 130$	$\nu_{12} = 0.3$	$G_{12} = 8$	$\rho = 1580$
$E_2 = 9$	$\nu_{23} = 0.26$	$G_{23} = 6.3$	
$E_3 = 9$	$\nu_{13} = 0.3$	$G_{13} = 8$	

Calculus of dispersion curves for composite plates is unanimously considered a difficult issue (Moser *et al.*, 1999; Sorohan *et al.*, 2011). In this case, a 2D application that models plane strain in the Z direction with PLANE42 type finite elements was considered. The dispersion points, obtained only for Lamb wave length less than 30 mm and wave frequency less than 1.2 MHz, were plotted in Fig. 15. The calculated group velocity was obtained with a method described in Sorohan *et al.* (2011), for a perturbation of 2.5% of the initial lengths.

Having in view that around the frequency of 300 kHz only quasi non-dispersive fundamental S0 and A0 modes are propagating, that value was

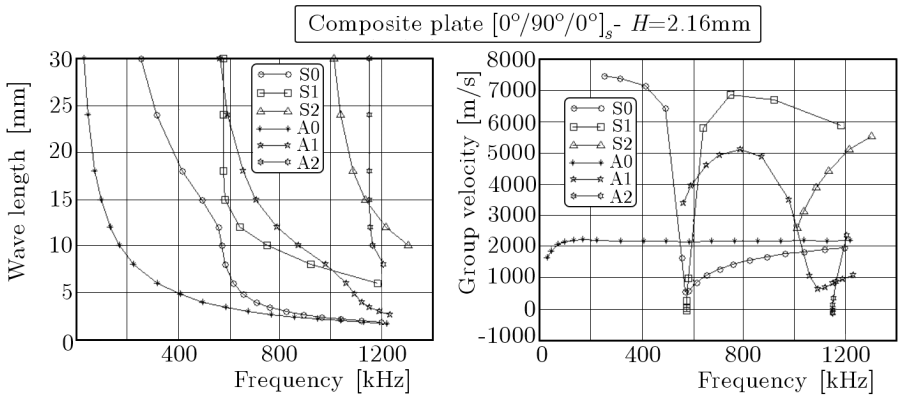

Fig. 15. Dispersion curves for a 2.16 mm thick, $[0/90/0]_s$ cross-ply composite plate, in plane strain condition, in the 0° direction

chosen as central frequency for Lamb wave actuation. The wavelength λ and the group velocity v_g for each mode, in the 0° direction, are:

- for S0: $\lambda = 25\,\text{mm}$ and $v_g = 7200\,\text{m/s}$
- for A0: $\lambda = 6.5\,\text{mm}$ and $v_g = 2150\,\text{m/s}$.

That frequency was also a compromise between lower frequencies, at which the higher wave length allows a coarser mesh, easier to run, but avoiding detection of small flaws, and higher frequencies at which additional S1 and A1 modes have to be managed, and where the finer mesh necessary for proper description of the wave length allows detection of smaller flaws, by increasing the time of the analysis.

As propagation of Lamb modes is better described by models built with 8-node brick elements – Solid 164 in Ansys/LS Dyna – the composite panel was modelled with this type of elements. Having in view the wave length of the fundamental modes, mentioned before, and the largely agreed condition of allocating at least eight finite elements to every wave for appropriate modelling of wave propagation (Mace and Manconi, 2008), it resulted in the upper limit of 1 mm for the dimension of the finite element. The composite panel considered in the study (see Fig. 14) is large enough to imply a huge FE model that uses such elements. It was conceived with double symmetry, so that the study of a quarter of it becomes possible and feasible. In the quarter model, the axis of symmetry acts like true boundaries, so that the quadruple damage was considered away from the central zone of each quarter in order to avoid stunning interferences in that zone.

The quarter model was meshed with 395 290 nodes, defining 335 940 finite elements with an average 0.625 mm dimension. The central actuator kept the size of that used for the Al panel, and the Lamb waves were considered actuated by a similar distribution of uniform interface forces (Fig. 16). In fact, this is an approximation which optimistically considers the quasi-isotropic effect of the cross-ply sequence. The true distribution of the interface forces, due to the material local marked orthotropy meant to improve the structural only model cited before, has to be established in a separate study.

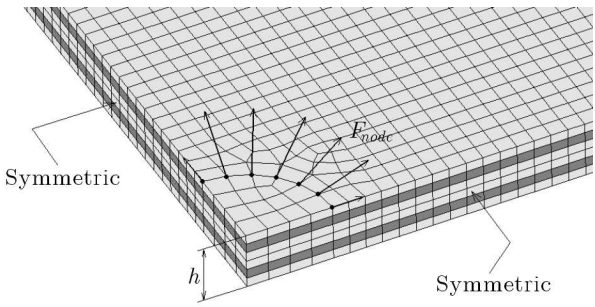

Fig. 16. Mesh, boundary conditions and interface actuation forces for the reduced model of the damaged composite panel

The actuation signal was defined with the same Hanning windowed force function (2.1), in which the parameters were changed to $F_0 = 5\,\mathrm{N}$, $n_0 = 3$ and $f_0 = 300\,\mathrm{kHz}$. In the small points marked as "sensor", the mid-plane displacements were extracted for catching the waves: the in-plane UX and UY displacements for S0 and the normal UZ displacement for A0. Reception of signals in each point was made using a function representing an extension of expression (2.2) in 3D

$$S = \operatorname{sgn}(u + v + w)\sqrt{u^2 + v^2 + w^2} \tag{3.1}$$

The damaged area was firstly considered to be 18 mm in diameter and modelled by 1000 times diminishing the elastic constants. As no effect on the propagation of Lamb waves was observed, the damaged area was increased to 31.25 mm in diameter (Fig. 17) and its severity also enhanced by 10 000 times diminishing the elastic constants. In Figs. 18 and 19, the images of wave propagation in the model in undamaged and damaged state, at the relevant moments are presented. These results are accompanied by diagrams showing the time history of the signals recorded in three relevant points. There is no evidence of echo signals (Fig. 20a,b) of signal attenuation (Fig. 20c) produced by the damaged area.

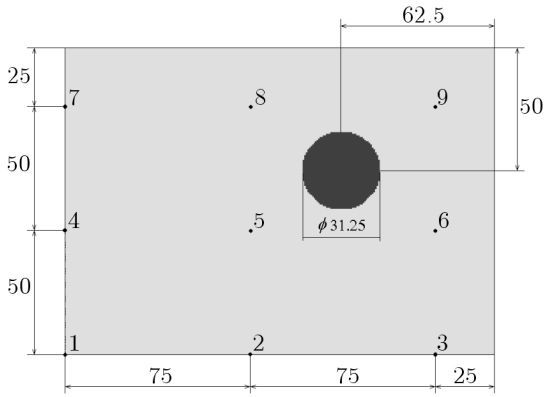

Fig. 17. The final location of the damaged area in the reduced model of the composite panel

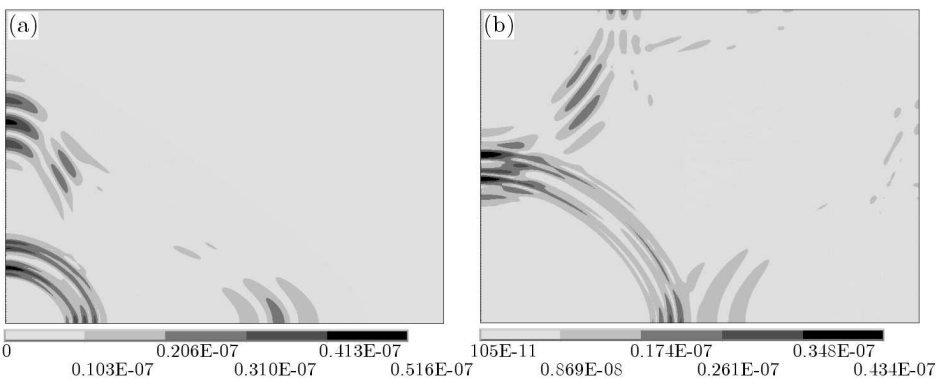

Fig. 18. Propagating waves at $t = 20\,\mu$s (a) and $t = 40\,\mu$s (b) in the pristine composite panel

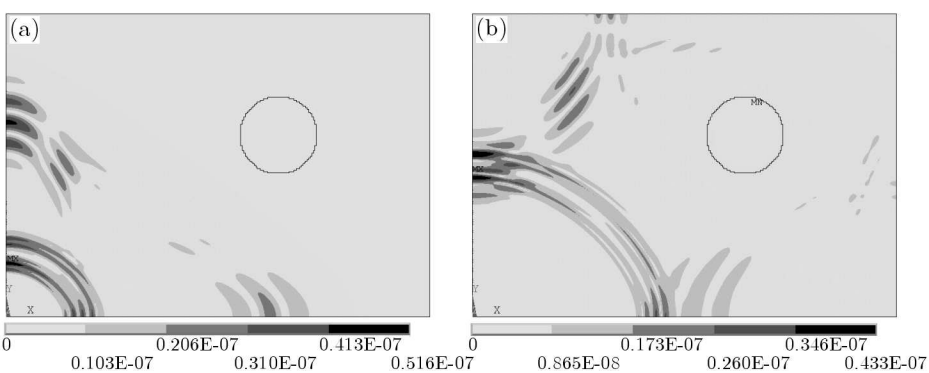

Fig. 19. Propagating waves at t $t = 20\,\mu$s (a) and $t = 40\,\mu$s (b) in the damaged composite panel

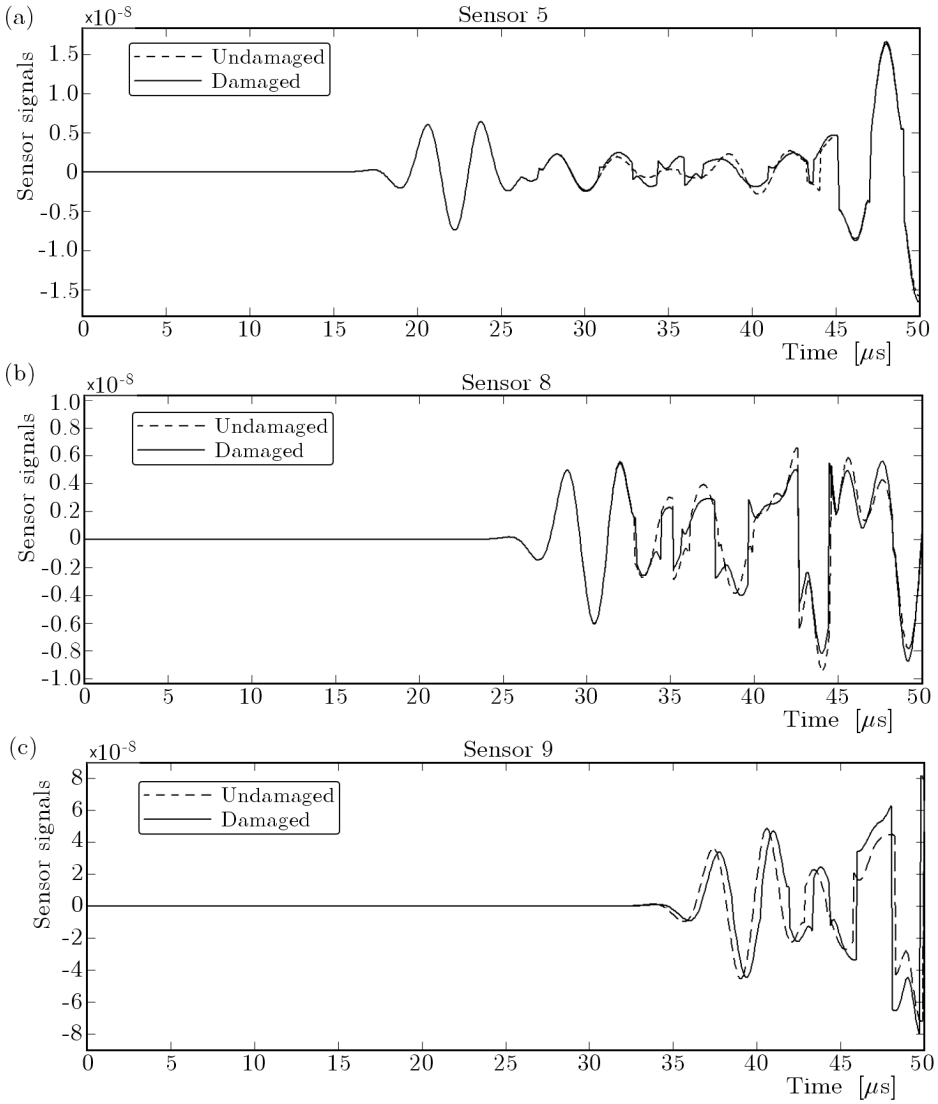

Fig. 20. Signals received in point 5 (a), point 8 (b) and point 9 (c) of the composite panel

4. Conclusions

The results presented in this paper and some others obtained during this same research work show, once again, that the Lamb wave method is still much easier to tackle on metals than on composites. Taking into consideration the present simulation, structural health monitoring of the Al or, normally,

of any metallic panel can be made quite easily with a simple inexpensive network of PZTs, following the above described pulse-echo type algorithm. For the localization process, much less complicated than in the cited works using sensor networks, it is essential to have a PZT patch with combined actuator-sensor functions in the middle of the panel, otherwise the ToF of the echo signal to every triangulation reference point cannot be easily deducted. Three other points, like points 6 and 15, used in this example, and point 13, to better catch the echo signals if damage is located on the left side of the panel, are enough for establishing the damage position with good accuracy. Such topology for the sensing points, close to the axis of symmetry and to the edges, avoids echo signal interference with powerful reflections from boundaries and sound definition of the triangle needed for having unique intersection of the range circles. Concerning that echo signal, it must be retained that only important damage creates detectable echo signals. These quite severely damaged areas can be detected and localized with that methodology allowing on-line inspection, then be evaluated with local SHM methods for actions to follow: repair or replacement.

The complex structure of the composite panel needs huge numerical models for realistic simulations. The reduced models, aimed to reduce the computation effort in conditions that other requirements, like the element dimensions, can be fulfilled, are creating additional difficulties, concerning mainly the reflected signals. The use of numerical non-reflective conditions on the boundaries aligned with the axes of symmetry did not offer better results, but produced further unexpected problems. The length of the blast signal must also be very carefully chosen, in relation with the reflected or echo signals and the range of possible excited modes. The wavelet transform or hard filtering in experimental simulation will be assessed as solutions to get a detectable echo signal in the future research work.

There are still refinements which must be added to the numerical models, like the modelling of the actuation of Lamb waves and the modelling of the damaged area, especially in the composite panel. Spectral Element Method (SEM) is increasingly used, but direct confrontation in accuracy and efficiency with more traditional approaches is still under way. All progress towards advanced numerical modelling/simulation must be done in close relation with experiments, which will certify robust and reliable models, able to offer trusting data about damage location and, in the next step, about its severity.

Acknowledgement

The research work was supported from a grant awarded by Romanian Ministry of Education, Research, Youth and Sports.

References

1. Burgos D.A.T., Mujica L.E., Güemes A., Rodellar J., 2010, Active piezoelectric system using PCA, *Proc. Fifth European Workshop Structural Health Monitoring*, 164-169
2. Cawley P., Alleyne D., 1996, The use of Lamb waves for the long-range inspection of large structures, *Ultrasonics*, **34**, 2, 287-290
3. Cheng L., Su Z., Yu L., 2010, Evaluation of structural damage using Correlative Sensor Array (CSA), *Proc. Fifth European Workshop Structural Health Monitoring*, 444-450
4. Constantin N., Sorohan Ş., Anghel V., Găvan M., 2006, Finite element analysis on the mechanism of Lamb wave generation with piezoelectric transducers, *Proc. Int, Semiconductor Conf. (CAS 2006)*, **2**, 403-406
5. De Stefano M., Gherlone M., Mattone M., Di Sciuva M. Worden K., 2010, On sensor placement for impact location: optimization under the effect of uncertainties, *Proc. Fifth European Workshop Structural Health Monitoring*, 402-407
6. Diamanti K., Soutis C., Hodgkinson J.M., 2007, Piezoelectric transducer arrangement for the inspection of large composite structures, *Composites A*, **38**, 4, 1121-1130
7. Diaz Valdes S.H., Soutis C., 2000, Health monitoring of composites using Lamb waves generated by piezoelectric devices, *Plastics, Rubber and Composites*, **29**, 9, 475-481
8. Giurgiutiu V., 2008, *Structural Health Monitoring with Piezoelectric Wafer Active Sensors*, Academic Press, an imprint of Elsevier, Burlington, MA
9. Ihn J.-B., Chang F.-K., 2009, Baseline-free Imaging Method based on New PZT Sensor Arrangements, *Journal of Intelligent Material Systems and Structures*, **20**, 1663-1673
10. Kessler S.S., Spearing S.M., Soutis C., 2002, Damage detection in composite materials using Lamb waves, *Smart Mat. Structures*, **11**, 2, 269-278
11. Lu Y., Su Z., Ye L., 2006, Crack identification in aluminium plates using Lamb wave signals of a PZT sensor network, *Smart Materials and Structures*, **15**, 3, 839-849
12. Mace B.R., Manconi E., 2008, Modelling wave propagation in two-dimensional structures using finite element analysis, *Journal of Sound and Vibration*, **31**, 8, 884-902
13. Moser F., Jacobs L.J., Qu J., 1999, Modeling elastic wave propagation in waveguides with the finite element method, *NDT&E International*, **32**, 225-234

14. NAYFEH A.H., 1991, The general problem of elastic wave propagation in multilayered anisotropic media, *Journal of Acoustic Society of America*, **89**, 4, 1521-1531

15. NIEUWENHUIS J.H., NEUMANN J., GREVE D.W., OPPENHEIM I.J., 2005, Generation and detection of guided waves using PZT wafer transducers, *IEEE Trans. Ultrasonics, Ferroelectrics, and Frequency Control*, **52**, 11, 2103-2111

16. OSTACHOWICZ W., KUDELA P., MALINOWSKI P., WANDOWSKI T., 2009, Damage localisation in plate-like structures based on PZT sensors, *Mechanical Systems and Signal Processing*, **23**, 6, 1805-1829

17. PADULA S.L., KINCAID R.K., 1999, Optimization strategies for sensor and actuator placement, Technical Report LA-13070-MS, NASA-Langley Research Center, Hampton, Virginia

18. PAGET C.A., TIPLADY K., KLUGE M., BECKER T., SCHALK J., 2010, Feasibility study of wireless impact damage assessment, *Proc. Fifth European Workshop Structural Health Monitoring*, 125-130

19. PAPADIMITRIOU C., 2005, Pareto optimal sensor locations for structural identification, *Computer Methods in Applied Mechanics and Engineering*, **194**, 12/16, 1655-1673

20. RICCI F., MONACO E., TANCREDI S., LECCE L., BANERJEE S., MAL A.K., 2010, Vibration and ultrasonic based methodologies for damage detection, *Proc. Fifth European Workshop Structural Health Monitoring*, 510-516

21. SOROHAN Ş., CONSTANTIN N., ANGHEL V., GĂVAN, M., 2007, Finite element analysis of generation and detection of Lamb waves using piezoelectric transducers, [In:] *Mathematics in Industry*, **11**, Eds. G. Ciuprina and D. Ioan, Springer-Verlag, Berlin, Heidelberg, 89-96

22. SOROHAN Ş., CONSTANTIN N., GĂVAN M., ANGHEL V., 2011, Extraction of dispersion curves for waves propagating in free complex waveguides by standard finite element codes, *Ultrasonics*, **51**, 503-515

23. TSUTSUI H., HIRANO N., KIMOTO J., AKATSUKA T., SASHIKUMA H., TAKEDA N., KOSHIOKA Y., 2010, Practical application study of an impact damage detection system for an airframe composite structure, *Proc. Fifth European Workshop Structural Health Monitoring*, 170-176

24. TUA P.S., QUEK S.T., WANG Q., 2004, Detection of cracks in plates using piezo-actuated Lamb waves, *Smart Materials and Structures*, **13**, 4, 643-660

25. VON ENDE S., LAMMERING R., 2009, Modeling and simulation of Lamb wave generation with piezoelectric plates, *Mechanics of Advanced Materials and Structures*, **16**, 3, 188-197

26. WANDOWSKI T., MALINOWSKI P., OSTACHOWICZ W., 2010, Comparison of distributed and concentrated networks of piezoelectric transducers, *Proc. Fifth European Workshop Structural Health Monitoring*, 704-711

27. Wang X., Lu Y., Tang J., 2008, Damage detection using piezoelectric transducers and the Lamb wave approach: I. System analysis, *Smart Materials and Structures*, **17**, 2, doi: 10.1088/0964-1726/17/2/025033

28. Zhongquing S., Lin Y., Ye L., 2006, Guided Lamb waves for identification of damage in composite structures: A review, *Journal of Sound and Vibration*, **295**, 3/5, 753-780

29. *ANSYS Structural Analysis Guide*, 2003, 3rd Edition, SAS IP

Efektywny i ekonomiczny układ sieci piezoelektryków do detekcji i lokalizacji uszkodzeń słabo zakrzywionych paneli

Streszczenie

W artykule zaprezentowano rezultaty badań dotyczących opracowania efektywnej metody inspekcji materiałów opartej na zastosowaniu fal Lamba wytwarzanych silnym centralnym generatorem sygnału oraz układem sieci czujników umożliwiającym wprowadzenie algorytmu triangulacji do wykrywania i lokalizowania uszkodzeń w panelach metalicznych i kompozytowych. Zbadano dwa warianty realizacji tego celu: (i) poprzez naklejenie centralnego wzbudnika piezoceramicznego pozwalającego wygenerować wielokierunkową falę o zadanej częstotliwości, kształcie i czasie trwania, (ii) poprzez użycie mobilnego aktuatora o sterowanym kącie działania zdolnego do wytworzenia silnej fali prowadzonej. Pierwszy wariant jest przewidziany do ciągłego monitoringu konstrukcji, drugi do badań w terenie. Na obecnym etapie zrealizowano jedynie badania symulacyjne dla pierwszego wariantu, otrzymując obiecujące wyniki w przypadku paneli metalicznych.

Manuscript received February 28, 2011; accepted for print April 6, 2011